ACS OMEGA

Article

Cite This: ACS Omega 2019, 4, 6044−6049

http://pubs.acs.org/journal/acsodf

Optical Stability of 1,1′-Binaphthyl Derivatives

Nikolay V. Tkachenko and Steve Scheiner*

Department of Chemistry and Biochemistry, Utah State University, Logan, Utah 84322-0300, United States

Supporting Information

ABSTRACT: The racemization process of various 1,1′-binaphthyl derivatives is studied by quantum calculations. The preferred racemization pathway passes through a transition state belonging to the C_i symmetry group. The energy barrier for this process is independent of solvation, the electron-withdrawing/releasing power of substituents, or their ability to engage in H-bonds within the molecule. The primary factor is instead the substituent size. The barrier is thus reduced when the −OH groups of 1,1′-bi-2-naphthol are replaced by H. There is a drop in the barrier also when the substituents are moved from the 2,2′ positions to 6,6′, where they will not come close to one another in the transition state. Upon removal of the peripheral aromatic rings of the binaphthyl system, the biphenyl system undergoes a facile racemization. It is concluded that the optimal means of improving optical stability of 1,1′-binaphthyl systems is the substitution of large bulky groups in the 2,2′ positions.

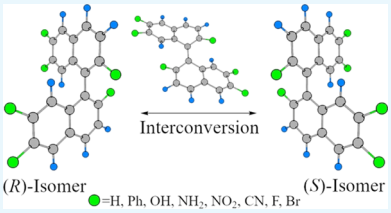

INTRODUCTION

Due to its high optical stability, molecules containing the 1,1′-binaphthyl skeleton (Figure 1) have found wide applications in various enantioselective processes for several decades. In particular, 1,1′-bi-2-naphthol (or BINOL) is widely used for asymmetric catalysis,[1,2] for chiral recognition processes,[3] and as a progenitor of chiral binaphthyl polymers.[4] Over the past half century, a huge number of effective methods have been developed to obtain optically pure BINOL isomers, including those utilizing chemical[5−7] and enzymatic resolution of racemic BINOLs,[8−10] as well as various catalytic procedures implementing Cu-,[11−13] V-,[14−16] Ru-,[17] and Fe-based[18,19] catalysts for direct asymmetric oxidative coupling of 2-naphthols.

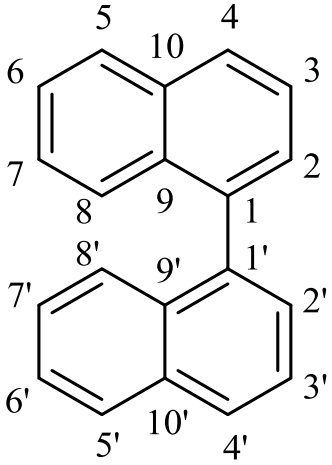

Figure 1. Structure of 1,1′-binaphthyl, including atomic numbering.

The high optical stability of these molecules revolves around the high energy barrier for their racemization. However, despite the wide use of binaphthyl derivatives, the racemization process of these compounds has not been fully explored. There have been some computational efforts in this direction.[20−26] In 1963, Cooke and Harris suggested two possible anti pathways of the racemization process of 1,1′-binaphthyl derivatives.[35] Later, Carter and Liljefors introduced two possible syn pathways.[24] However, these racemization routes were investigated only via very approximate molecular mechanics and semiempirical methods. The computationally predicted value of the racemization barrier for the anti-C_i TS of 1,1′-binaphthalene lies in the 18.3−24.8 kcal/mol interval, depending upon the level of theory. The most recent and accurate result (23.0 kcal/mol) was obtained using the B3LYP/6-31G(d,p) level of theory.[22] Previous theoretical analyses agree that the anti-C_i pathway is preferred. Schleyer and co-workers made the assumption that the distortion of the aromatic rings makes the greatest contribution to the activation energy of the process,[21] which was echoed later by Havlas et al.[22] Experimental measurements of the optical stability of 1,1′-binaphthyl[22,27−30] in different solvents suggest only slight sensitivity of the racemization energy barrier to the particular solvent, varying in the narrow range between 23.5 and 24.1 kcal/mol. For the −OH-substituted 1,1′-bi-2-naphthol, the activation free energy of the racemization process in naphthalene and diphenyl ether is a bit higher, at 37.2 and 37.8 kcal/mol, respectively.

There remain some interesting and fundamental question as to why this barrier is so high. Is this an electronic effect or is it related to the steric interactions during racemization? Are there present any noncovalent interactions that impede or facilitate the conversion from one optical isomer to another? What is the precise path of molecular arrangement that accompanies the

Received: March 5, 2019
Accepted: March 11, 2019
Published: March 29, 2019

DOI: 10.1021/acsomega.9b00619
ACS Omega 2019, 4, 6044−6049

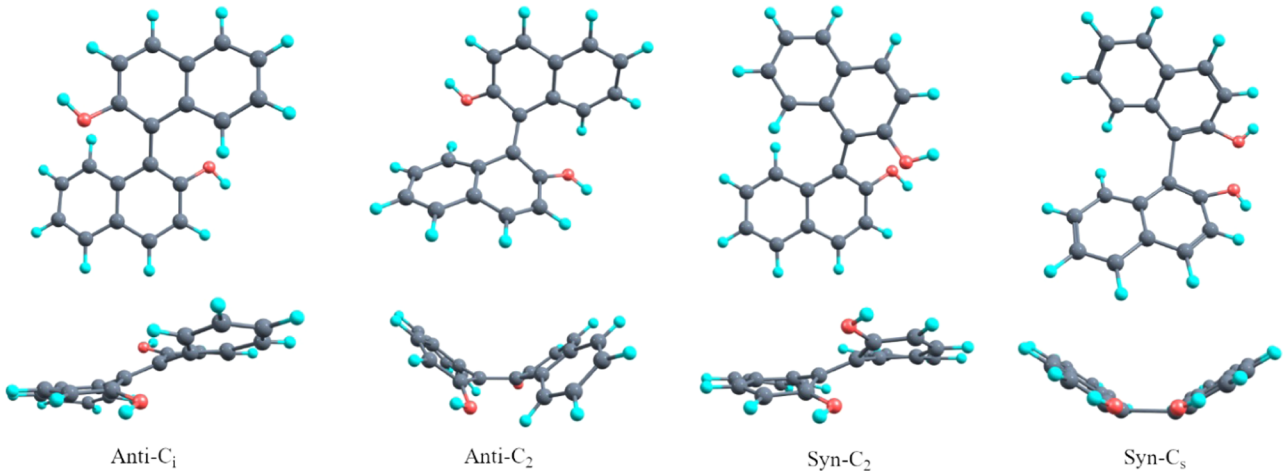

Figure 2. Top and side views of racemization pathways of BINOL.

racemization? What sorts of substituents might compromise the optical stability by lowering the barrier, or might add to it via raising the barrier even higher?

The current work describes a quantum chemical investigation of these questions. A thorough examination of the entire potential energy surface leads to the likely racemization pathway and elucidates the structure of the transition state along this reaction profile. Various substituents are added that allow identification of the components that contribute to the racemization barrier and suggest modifications of the molecular skeleton that would add to or subtract from the optical stability.

METHODS

Full geometry optimizations were performed at various levels of theory. For 1,1′-bi-2-naphthol geometry optimization and frequency calculations (harmonic approximation), three density functional theory (DFT) methods were used (PBE0,[32] B3LYP,[33−35] and TPSSh[36]) with Pople augmented basis set 6-311+G*. For a more accurate accounting of electron correlation, the MP4/cc-pVDZ//B3LYP/6-311+G* level of theory was implemented. Transition state structures were identified using a synchronous transit-guided quasi-Newton method.[31] Optimization of displaced geometry along the reaction coordinate ensured that each transition state truly refers to the racemization process. For investigating substituent effects, the B3LYP/6-311+G* level of theory was applied. All energies in this work are presented with the zero-point energy (ZPE) corrections included. (Coordinates of optimized geometries are contained in the Supporting Information (SI) as well as energetics without ZPE correction and free energies.) All calculations utilized the Gaussian-09[37] and Gaussian-16[38] programs. The ChemCraft 1.8 program was used for structure visualization. Charge transfer between individual orbitals was measured by the natural bond orbital (NBO) protocol.[39,40] Atoms in molecules (AIM) procedures[41,42] as implemented in the MultiWFN code were used for the elucidation of bonding paths between atoms and for the quantification of the electron density at bond critical points.

RESULTS AND DISCUSSION

To facilitate discussion of the results, the following notation is adopted. The peripheral six-membered rings are those not engaged in a covalent bond between the two naphthyl systems, containing C5−C8 and C5′−C8′ (Figure 1). When these two peripheral rings lie on the same side of the C1−C1′ bond, as they do in Figure 1, this sort of geometry is designated as syn. A 180° rotation around the C1−C1′ bond results in an antistructure. In addition to this general distinction, there is also the precise symmetry adopted by the transition state along the pathway. The four transition state geometries for the BINOL molecule are displayed in Figure 2, along with their designations, which include the TS point group. (The same notation was used in a previous study of binaphthyl racemization pathways.[22]) It should be added that in some cases the presence of substituents will remove the strict symmetry described above, but this notation will be applied nonetheless for purposes of consistency.

Given the freedom of rotation around the −OH bonds of BINOL, the three most likely isomers of this molecule are illustrated in Figure 3 for the (R)-enantiomer.[43] One would anticipate that isomer **A** ought to be the most stable, containing as it does the possibility of two internal OH···O H-bonds. Indeed, calculations confirm **A** to be more stable than **B**, with its single such H-bond by 3.8, and **C** by 6.9 kcal/mol since the latter contains no such bond. Transformation between the isomers in Figure 3 is facile. The energy barrier for

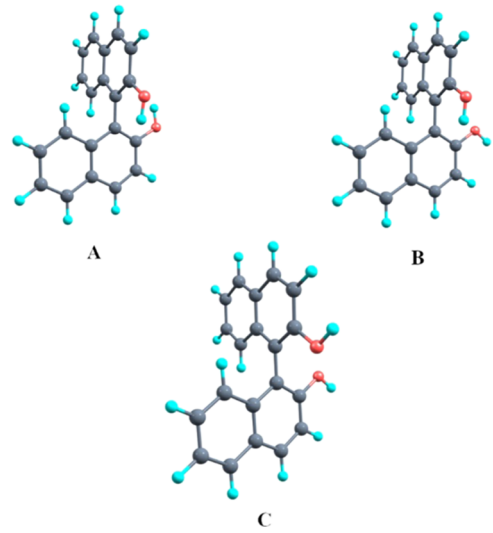

Figure 3. Isomers of (*R*)-1,1′-bi-2-naphthol.

DOI: 10.1021/acsomega.9b00619
ACS Omega 2019, 4, 6044−6049

Table 1. Transition State Energies (kcal/mol) of 1,1′-Bis-2-naphthol[a]

isomer	TS-type	B3LYP 6-311+G*	TPSSh 6-311+G*	PBE0 6-311+G*	MP2 cc-pVDZ	MP3 cc-pVDZ	MP4 cc-pVDZ
A	anti-C_i	39.3	37.0	38.7	36.3	39.7	35.8
	syn-C_2	43.2	41.2	42.9	40.9	43.3	40.0
B	syn-C_2	42.2	43.0	44.0	40.3	42.7	39.5
C	anti-C_i	39.5	37.6	39.0	37.6	40.3	36.9
	anti-C_2	52.2	50.6	52.6	52.0	54.3	50.6
	syn-C_2	40.8	39.1	40.5	39.3	41.3	38.5

[a]All energies are indicated relative to the energy of the optimized geometry of the corresponding isomer, with geometries optimized at noted levels.

B collapsing to **A** is only 1.7 kcal/mol, whereas there is no effective barrier for the transition from **C** to **B**.

Even though **C** is unlikely to exist in any large proportion, and the transition from **B** to **A** requires surmounting only a small barrier, in the interest of thoroughness, the barriers to racemization were calculated for all three isomers and are listed in Table 1. A first observation concerns the insensitivity of the data to the level of theory. The barrier to conversion of the **A** isomer through the anti-C_i transition state, for example, lies in the narrow range between 37.0 and 39.7 kcal/mol regardless of the DFT functional or the incorporation of electron correlation via any level of Møller−Plesset perturbation (MPn) theory.

It may be noted that not all of the starting isomers pass through each of the four possible transition states. Isomer **A**, for example, pass through only the anti-C_i and syn-C_2 transition states. However, in any case, the overall conclusion is that the preferred pathway lies through the anti-C_i structure, with a barrier of just under 40 kcal/mol. This finding conforms to an earlier hypothesis.[22] It is noteworthy that energy barriers of each of the different isomers are roughly the same. One may presume that, given the low energy barrier separating **B** from **A**, the most likely racemization process of the former would take it through **A** and its anti-C_i transition state.

These energetics of the various conversion routes are presented graphically in Figure 4, in which the energies of the

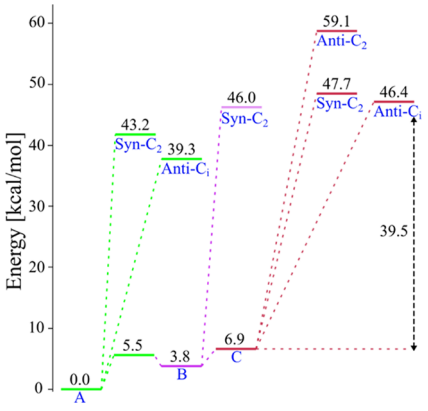

Figure 4. Energy diagram of BINOL isomers and transition states, calculated at the B3LYP/6-311+G* level.

various pathways can be directly compared. The energy of the anti-C_i transition state for the **A** isomer lies lower by 7.1 kcal/mol as compared to that of the same symmetry transition state for the **C** structure. To probe the reasons for this energy advantage, both AIM and NBO were applied to the two structures. Figure 5 indicates the position of a pair of bond paths connecting the OH proton with the C atom of the phenyl ring of **A**. These paths are replaced in **C** by a similar pair in which it is the hydroxyl O atom that connects with the

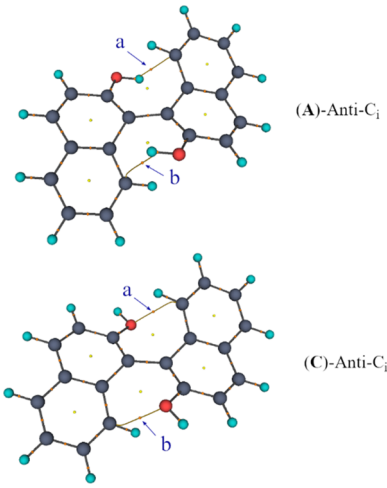

Figure 5. AIM bond paths and bond critical points for anti-C_i transition states of isomers **A** and **C**.

phenyl C atom. The AIM analysis might term these interactions a OH···C H-bond and a O···C tetrel bond, respectively. The electron densities for the bond critical points in the **A** TS are equal to 0.0241 and 0.0195, which compared to 0.0217 for both of the **C** bond paths are quite similar. The NBO analysis suggests a significant degree of charge transfer (with $E(2)$=1.97 kcal/mol) from a π(CC) bonding orbital of the phenyl ring to the σ^*(OH) bond in the **A** TS, indicative of a OH···π H-bond. For the **C** isomer, a charge transfer ($E(2)$ =1.63 kcal/mol) occurs from the O lone pair to the π^*(CC) of the phenyl ring, which is likely attributable to a tetrel bond. These results suggest that the difference in energy between the **A** and **C** transition states is not due to these intramolecular contacts but due to some other factors, as described below.

It is important to consider the optical stability of BINOL not just in vacuo but also in a solvent environment. Accordingly, the energies of the two transition states of the **A** isomer were assessed in two different solvents. The dielectric constants of diphenyl ether and *N*,*N*-dimethylformamide are equal to 3.73 ad 37.22, respectively, thus representing a fairly wide range of this parameter. Within the context of the former solvent, the energies of the anti-C_i and syn-C_2 transition states, relative to the optimized **A** isomer, are 39.6 and 43.3 kcal/mol, respectively, quite similar to the gas phase values of 39.3 and 43.2 kcal/mol. Increasing the dielectric constant to 37.2 also has a little effect, with activation barriers of 39.8 and 43.3 kcal/mol. The insensitivity of this quantity to solvation suggests that there is little differentiation between the equilibrium and transition state structures in terms of charge separation, adding to the argument that electronic effects are not a primary factor in the barrier to racemization.

DOI: 10.1021/acsomega.9b00619
ACS Omega 2019, 4, 6044−6049

Substituents. To probe this issue more deeply, the next question arises with regard to the effect of the −OH groups of the BINOL molecule upon its optical stability. By removing these groups, one can obtain a pure representation of the rotational profile of the basic 1,1′-binaphthyl skeleton. Similarly, by replacing −OH with a number of other groups, it would be possible to learn about how both electronic and steric effects might enter into the picture. As the calculations of BINOL at various levels described above have shown little sensitivity to the level of theory, the following results were extracted from application of B3LYP/6-311+G*, which nicely reproduces the data from more complete calculations.

The nature of the potential energy surface is such that the search for transition states is not always successful. It was only possible to identify such geometries for certain substituents for the anti-C_2 structure, whereas none could be found for syn-C_s. However, even with the incomplete set of data presented in Table 2, it is nonetheless possible to extract key features of the

Table 2. Transition State Energies[a] (kcal/mol) of 2,2′ Disubstituted 1,1′-Binaphthyls as Well as Experimental Data of Rotational Barrier

TS-type	−H	−OH (A)	$-NH_2$	$-NO_2$	−F	−CN	−Ph
anti-C_i	19.5	39.3	42.2	41.1	36.5	40.9	43.5
anti-C_2	26.0[b]	−[c]	−[c]	−[c]	48.1	57.0	−[c]
syn-C_2	27.9	43.2	44.4	44.7	38.4	41.8	43.9
exp.	23.5[27]	37.8[22]	42.5[47]	–	–	–	–
B val.[46]	–	<5.0	8.1	7.6	<5.0	–	–

[a]All energies are indicated relative to the energy of the optimized geometry of the corresponding isomer, with geometries optimized at the B3LYP/6-311+G* level. [b]Second-order stationary point. [c]Structure cannot be located at this level of theory.

sensitivity of the activation energy to the nature of the substituent. Considering the anti-C_i data in the first row of the table, the removal of the −OH substituent, replacing it by H, drops the barrier to roughly half its value. On the other hand, all of the substituents are associated with barriers in the surprisingly narrow range of 36.5−43.5 kcal/mol. There is little correlation between the barrier and electron-withdrawing or -releasing character of R. For example, the strongly electron-releasing $-NH_2$ shows nearly the identical barrier as the electron-withdrawing $-NO_2$. It would appear, then, that the dominating characteristic is the size of the substituent. Previous theoretical results obtained for large substituents are consistent with this assumption (computed rotational barriers for 2,2′-bis(diphenylphosphino)-1,1′-binaphthyl and 2-amino-2′-hydroxy-1,1′-binaphthyl are 49.4[44] and 40.4[45] kcal/mol, respectively). The barrier for H is by far the lowest, whereas the highest barrier occurs for the bulky phenyl group. The relatively small size of the monatomic F leads to the lowest barrier (with the exception of H of course). Very similar trends are observed in the case of the syn-C_2 transition states. Qualitatively, such behavior is consistent with the *B* parameter proposed by Schlosser.[46] The main idea of this approach is to rank substituents as a function of steric congestion. Following this concept, one could predict the relative energy of rotational barrier for 2,2′ disubstituted 1,1′-binaphthyls.

By placing the substituent on the peripheral pair of rings, the ones that do not form covalent attachment between the two naphthyl systems, it is possible to examine electronic effects without the strong influence of steric factors. The effects of 6,6′ substitution upon the racemization barriers are reported in Table 3. Again, the identification of transition states for the

Table 3. Transition State Energies (kcal/mol) of 6,6′ Disubstituted 1,1′-Binaphthyls[a]

TS-type	−H	$-NH_2$	−F	−Br	−Ph
anti-C_i	19.5	24.6	24.8	24.4	24.1
anti-C_2	26.0[b]	30.9[b]	31.4[b]	30.9[b]	−[c]
syn-C_2	27.9	33.2	33.3	32.8	32.5

[a]All energies are indicated relative to the energy of the optimized geometry of the corresponding isomer, with geometries optimized at the B3LYP/6-311+G* level. [b]Second-order stationary point. [c]Structure cannot be located at this level of theory.

syn-C_2 geometry was difficult, leading to second-order stationary points. However, the data for the anti-C_i and syn-C_2 are unambiguous. As above for the 2,2′ substitution, the barriers for R═H are the smallest, but by less of a margin, only by 5 kcal/mol or so. Within the other substituents, the sensitivity to either electron-withdrawing power or even substituent size has all but disappeared. The barrier for the bulky Ph group is in fact even slightly smaller than that for the other R. In fact, what small differences that do occur are due not to the electronic energies but rather to zero-point vibrations. When the latter are removed, and it is only the electronic energies that are considered, the activation energies are virtually identical, even including R═H. Placement of the F substituent pair into the 3,3′ and 7,7′ positions leads to data quite similar to values in Table 3 for 6.6′.

Given what is apparently a dominating influence of steric repulsions on the racemization process, it is tempting to consider how this process would be affected if the peripheral rings were removed entirely, leaving only the 2,2′-biphenyl system. As one interesting difference, the transition states to the racemization of the smaller bisphenol system contain a pair of completely flat rings. That is, the ring nonplanarity, that is characteristic of the binaphthyl transition states, vanishes along with the peripheral rings. Second, and perhaps more importantly, the barriers to racemization are dramatically lowered. The barriers drop from 19.5 and 39.3 kcal/mol for binaphthyl and 1,1′-bi-2-naphthol, respectively, down to 2.4 and 11.2 kcal/mol for the corresponding biphenyl and 2,2′-biphenol. The removal of the peripheral rings, and the steric hindrance that they bring, thus reduces the optical stability of this system.

Since the major deformation of the aromatic system occurs in the phenyl rings that are directly attached to one another, the dihedral angle $\theta(1-9-4-3)$, shown in Figure 6, was taken

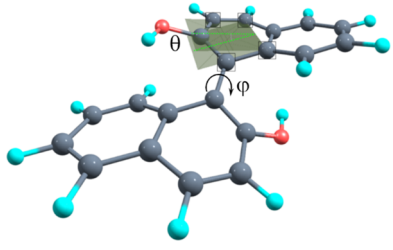

Figure 6. Dihedral angles θ, shown by green dotted lines, and φ representing the relative orientation of two aromatic systems.

DOI: 10.1021/acsomega.9b00619
ACS Omega 2019, 4, 6044−6049

Table 4. θ and φ Dihedral Angles for Substituted 1,1′-Binaphthyls

		2,2′ substituents							6,6′ substituents			
TS-type	angle	−H	−OH	$-NH_2$	$-NO_2$	−F	−CN	−Ph	$-NH_2$	−F	−Br	−Ph
anti-C_i	$\lvert\theta\rvert$	13.5	16.7	18.9	17.3	16.5	18.6	18.7	12.9	13.4	13.4	13.1
	$\lvert\varphi\rvert$	180.0	172.2	170.6	180.0	180.0	180.0	180.0	180.0	180.0	180.0	179.8
syn-C_2	$\lvert\theta\rvert$	13.6	18.0	19.4	17.8	16.2	17.5	14.7	13.0	13.5	13.4	13.4
	$\lvert\varphi\rvert$	27.0	25.6	30.3	10.2	25.0	2.6	28.2	26.6	27.1	27.1	26.9

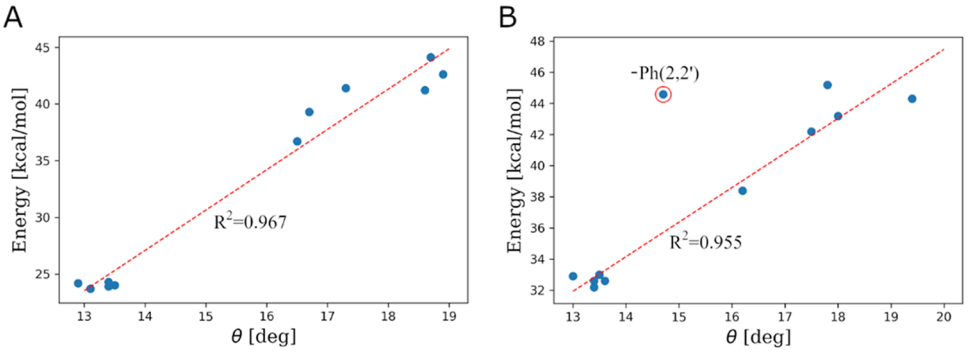

Figure 7. Nonplanarity angle θ vs relative electronic energies (without ZPE corrections) for anti-C_i isomers (**A**) and syn-C_2 isomers (**B**).

as a measure of this nonplanarity. This angle would be 0° for a completely planar system. The dihedral angle $\varphi(2-1-1'-2')$ characterizes the relative orientations of the two aromatic systems.

The values of these angles are displayed in Table 4 for the anti-C_i and syn-C_2 transition state structures with various substituents. φ is equal to 180° for the anti-C_i pathway for all cases except −OH(2,2′) and $-NH_2$(2,2′) substituents. This approximately 8−9° deviation suggests some involvement of H-bonds. This same angle is equal to roughly 30° for most of the syn-C_2 transition states, with the exception of the $-NO_2$ and −CN substituents, where it is closer to planar. An intriguing correlation is observed between the nonplanarity angle θ and the transition state energy. As illustrated in Figure 7, the energy rises as nonplanarity is introduced into this aromatic system. There is one outlier, in that the −Ph(2,2′) substituent falls off this linear relationship (and excluded from the linear approximation sample), which is attributed to the close proximity of the two phenyl groups along the syn-C_2 pathway, which is in turn accompanied by additional repulsive interactions.

CONCLUSIONS

The racemization of BINOL and its variations with a 1,1′-binaphthyl skeleton passes through a preferred anti-C_i transition state. Replacement of H at the 2,2′ positions with any substituent, whether −OH as in BINOL or any other group, raises the barriers to racemization up to about 40 kcal/mol, leading to the optical stability of this series of molecules. This barrier is insensitive to the electron-withdrawing power of the substituents but depends to some extent on their bulkiness. Placing the substituents in the 6,6′ positions, where there are less steric repulsions between them, reduces the racemization barrier to only about 25 kcal/mol. Removal of the peripheral rings of the naphthyl systems, leaving only a biphenyl skeleton, reduces the barrier still further to 11 kcal/mol or less. It would appear that 2,2′ substitution, especially of large bulky groups, offers the optimal means of improvements in optical stability of the 1,1′-binaphthyl system.

ASSOCIATED CONTENT

Supporting Information

The Supporting Information is available free of charge on the ACS Publications website at DOI: 10.1021/acsomega.9b00619.

Energies of transition states of 1,1′-binaphthyl derivatives without ZPE correction; free energies of transition states of 1,1′-binaphthyl derivatives at 298 K; Cartesian coordinates of optimized geometries; total energies, number of imaginary frequencies; and value of ZPE corrections for all structures discussed above (PDF)

AUTHOR INFORMATION

Corresponding Author

*E-mail: steve.scheiner@usu.edu.

ORCID

Steve Scheiner: 0000-0003-0793-0369

Notes

The authors declare no competing financial interest.

REFERENCES

(1) Chen, Y.; Yekta, S.; Yudin, A. K. Modified BINOL Ligands in Asymmetric Catalysis. *Chem. Rev.* **2003**, *103*, 3155−3211.

(2) Brunel, J. M. Update 1 of: BINOL: A Versatile Chiral Reagent. *Chem. Rev.* **2007**, *107*, PR1−PR45.

(3) Pu, L. 1,1′-Binaphthyl Dimers, Oligomers, and Polymers: Molecular Recognition, Asymmetric Catalysis, and New Materials. *Chem. Rev.* **1998**, *98*, 2405−2494.

(4) Morgan, B. J.; Xie, X.; Phuan, P.-W.; Kozlowski, M. C. Enantioselective Synthesis of Binaphthyl Polymers Using Chiral Asymmetric Phenolic Coupling Catalysts: Oxidative Coupling and Tandem Glaser/Oxidative Coupling. *J. Org. Chem.* **2007**, *72*, 6171−6182.

(5) Brunel, J. M.; Buono, G. A New and Efficient Method for the Resolution of 1,1′-Binaphtha1ene-2,2′-diol. *J. Org. Chem.* **1993**, *58*, 7313−7314.

(6) Fabbri, D.; Delogu, G.; De Lucchi, O. A Widely Applicable Method of Resolution of Binaphthyls: Preparation of Enantiomerically Pure 1,1′-Binaphthalene-2,2′-diol, 1,1′-Binaphthalene-2,2′-di-

DOI: 10.1021/acsomega.9b00619
ACS Omega 2019, 4, 6044−6049

thiol, 2′-Mercapto-1,1′-binaphthalen-2-ol, and 1,1′-Binaphthalene-8,8′-diol. *J. Org. Chem.* **1995**, *60*, 6599−6601.
(7) Wang, M.; Liu, S. Z.; Liu, J.; Hu, B. F. Diastereoselective Synthesis of 1,1′-Binaphthy-2,2′-diol. *J. Org. Chem.* **1995**, *60*, 7364−7365.
(8) Wu, S.-H.; Zhang, L.-Q.; Chen, C.-S.; Girdaukas, G.; Sih, C. J. Bifunctional Chiral Synthons via Biochemical Methods.: VII. Optically-Active 2,2′-Dihydroxy-1,1′-Binaphthyl. *Tetrahedron Lett.* **1985**, *26*, 4323−4326.
(9) Kazlauskas, R. J. Resolution of Binaphthols and Spirobiindanols Using Cholesterol Esterase. *J. Am. Chem. Soc.* **1989**, *111*, 4953−4959.
(10) Gialih, L.; Shih-Huang, L.; Show-Jane, C.; Fang-Chen, W.; Hwey-Lin, S. "Triple Enantioselection" by an Enzyme-Catalyzed Transacylation Reaction. *Tetrahedron Lett.* **1993**, *34*, 6057−6058.
(11) Hewgley, J. B.; Stahl, S. S.; Kozlowski, M. C. Mechanistic Study of Asymmetric Oxidative Biaryl Coupling: Evidence for Self-Processing of the Copper Catalyst to Achieve Control of Oxidase vs Oxygenase Activity. *J. Am. Chem. Soc.* **2008**, *130*, 12232−12233.
(12) Alamsetti, S. K.; Poonguzhali, E.; Ganapathy, D.; Sekar, G. Enantioselective Oxidative Coupling of 2-Naphthol Derivatives by Copper-(R)-1,1′-Binaphthyl-2,2′-diamine-TEMPO Catalyst. *Adv. Synth. Catal.* **2013**, *355*, 2803−2808.
(13) Gao, J.; Reibenspies, J. H.; Martell, A. E. Structurally Defined Catalysts for Enantioselective Oxidative Coupling Reactions. *Angew. Chem.* **2003**, *115*, 6190−6194.
(14) Guo, Q.-X.; Wu, Z.-J.; Luo, Z.-B.; Liu, Q.-Z.; Ye, J.-L.; Luo, S.-W.; Cun, L.-F.; Gong, L.-Z. Highly Enantioselective Oxidative Couplings of 2-Naphthols Catalyzed by Chiral Bimetallic Oxovanadium Complexes with Either Oxygen or Air as Oxidant. *J. Am. Chem. Soc.* **2007**, *129*, 13927−13938.
(15) Luo, Z.; Liu, Q.; Gong, L.; Cui, X.; Mi, A.; Jiang, Y. Novel Achiral Biphenol-Derived Diastereomeric Oxovanadium(IV) Complexes for Highly Enantioselective Oxidative Coupling of 2-Naphthols. *Angew. Chem.* **2002**, *114*, 4714−4717.
(16) Somei, H.; Asano, Y.; Yoshida, T.; Takizawa, S.; Yamataka, H.; Sasai, H. Dual Activation in a Homolytic Coupling Reaction Promoted by an Enantioselective Dinuclear Vanadium(IV) Catalyst. *Tetrahedron Lett.* **2004**, *45*, 1841−1844.
(17) Irie, R.; Katsuki, T. Selective Aerobic Oxidation of Hydroxy Compounds Catalyzed by Photoactivated Ruthenium-Salen Complexes (Selective Catalytic Aerobic Oxidation). *Chem. Rec.* **2004**, *4*, 96−109.
(18) Egami, H.; Katsuki, T. Iron-Catalyzed Asymmetric Aerobic Oxidation: Oxidative Coupling of 2-Naphthols. *J. Am. Chem. Soc.* **2009**, *131*, 6082−6083.
(19) Tkachenko, N. V.; Lyakin, O. Y.; Samsonenko, D. G.; Talsi, E. P.; Bryliakov, K. P. Highly Efficient Asymmetric Aerobic Oxidative Coupling of 2-Naphthols in the Presence of Bioinspired Iron Aminopyridine Complexes. *Catal. Commun.* **2018**, *104*, 112−117.
(20) Tsuzuki, S.; Tanabe, K.; Nagawa, Y.; Nakanishi, H. Calculations of Internal Rotational Pathways of Peri Substituted Naphthalenes by Molecular Mechanics. *J. Mol. Struct.* **1990**, *216*, 279−295.
(21) Kranz, M.; Clark, T.; Schleyer, P. v. R. Rotational Barriers of 1,1′-Binaphthyls: A Computational Study. *J. Org. Chem.* **1993**, *58*, 3317−3325.
(22) Meca, L.; Řeha, D.; Havlas, Z. Racemization Barriers of 1,1′-Binaphthyl and 1,1′-Binaphthalene-2,2′-diol: A DFT Study. *J. Org. Chem.* **2003**, *68*, 5677−5680.
(23) Gamba, A.; Rusconi, E.; Simonetta, M. A Conformational Study of Phenyl- and Naphthyl-naphthalenes. *Tetrahedron* **1970**, *26*, 871−877.
(24) Carter, R. E.; Liljefors, T. A Theoretical Study of Configurational Inversion of 1,1′-Binaphthyl by Molecular Mechanics. *Tetrahedron* **1976**, *32*, 2915−2922.
(25) Liljefors, T.; Carter, R. E. The configurational inversion of methyl-substituted 1,1′-binaphthyls as studied by molecular mechanics. *Tetrahedron* **1978**, *34*, 1611−1615.
(26) Leister, D.; Kao, J. Theoretical Studies of Rotational Barriers in 1,1′-Biisoquinoline, 2,2′-Biquinoline and Substituted Styrenes, Alkenyl-Naphthalenes, and Alkyl-Binaphthyls. *J. Mol. Struct.: THEOCHEM* **1988**, *168*, 105−118.
(27) Cooke, A. S.; Harris, M. M. Ground-state strain and other factors influencing optical stability in the 1,1′-binaphthyl series. *J. Chem. Soc.* **1963**, 2365.
(28) Colter, A. K.; Clemens, L. M. Solvent Effects in the Racemization of 1,1′-Binaphthyl. A Note on the Influence of Internal Pressure on Reaction Rates. *J. Phys. Chem.* **1964**, *68*, 651.
(29) Kyba, E. P.; Gokel, G. W.; Jong, F.; Koga, K.; Sousa, L. R.; Siegel, M. G.; Kaplan, L.; Sogah, D. Y.; Cram, D. J. Host-Guest Complexation. 7. The Binaphthyl Structural Unit in Host Compounds. *J. Org. Chem.* **1977**, *42*, 4173.
(30) Cooke, A. S.; Harris, M. M. Optical Activity in the 1,1′-Binaphthyl Series. Energy Barriers to Racemisation of 8-Substituted 1,1′-Binaphthyls. *J. Chem. Soc. C* **1967**, 988−992.
(31) Peng, C.; Schlegel, H. B. Combining Synchronous Transit and Quasi-Newton Methods for Finding Transition States. *Isr. J. Chem.* **1993**, *33*, 449−454.
(32) Adamo, C.; Barone, V. Toward Reliable Density Functional Methods Without Adjustable Parameters: The PBE0 Model. *J. Chem. Phys.* **1999**, *110*, 6158−6170.
(33) Parr, R. G.; Yang, W. *Density-Functional Theory of Atoms and Molecules*; Oxford University Press: Oxford, 1989.
(34) Becke, A. D. Density-Functional Thermochemistry. III. The Role of Exact Exchange. *J. Chem. Phys.* **1993**, *98*, 5648.
(35) Perdew, J. P.; Chevary, J. A.; Vosko, S. H.; Jackson, K. A.; Pederson, M. R.; Singh, D. J.; Fiolhais, C. Atoms, Molecules, Solids, and Surfaces: Applications of the Generalized Gradient Approximation for Exchange and Correlation. *Phys. Rev. B* **1992**, *46*, 6671.
(36) Perdew, J. P.; Tao, J.; Staroverov, V. N.; Scuseria, G. E. J. Meta-Generalized Gradient Approximation: Explanation of a Realistic Nonempirical Density Functional. *J. Chem. Phys.* **2004**, *120*, 6898−6911.
(37) Frisch, M. J. et al. *Gaussian 09*, revision D.01; Gaussian, Inc., 2009.
(38) Frisch, M. J. et al. *Gaussian 16*, revision B.01; Gaussian, Inc., 2016.
(39) Foster, J. P.; Weinhold, F. Natural Hybrid Orbitals. *J. Am. Chem. Soc.* **1980**, *102*, 7211−7218.
(40) Reed, A. E.; Curtiss, L. A.; Weinhold, F. Intermolecular Interactions from a Natural Bond Orbital, Donor—Acceptor Viewpoint. *Chem. Rev.* **1988**, *88*, 899−926.
(41) Bader, R. F. W. *Atoms in Molecules, A Quantum Theory*; Clarendon Press: Oxford, U.K., 1990; Vol. *22*, p 438.
(42) Carroll, M. T.; Bader, R. F. W. An Analysis of the Hydrogen Bond in Base-HF Complexes Using the Theory of Atoms in Molecules. *Mol. Phys.* **1988**, *65*, 695−722.
(43) Sahnoun, R.; Koseki, S.; Fujimura, Y. Theoretical Investigation of 1,1′-Bi-2-Naphthol Isomerization. *J. Mol. Struct.* **2005**, *735*−*736*, 315−324.
(44) García, J. S.; Lepetit, C.; Canac, Y.; Chauvin, R.; Boggio-Pasqua, M. Enantiomerization Pathway and Atropochiral Stability of the BINAP Ligand: A Density Functional Theory Study. *Chem. Asian J.* **2014**, *9*, 462−465.
(45) Da, L.-G.; He, J.; Hu, L.-F. DFT Study on the Structure and Racemization Mechanism of 2-Amino-2′-Hydroxy-1,1′-Binaphthyl. *J. Phys. Org. Chem.* **2019**, *32*, No. e3900.
(46) Ruzziconi, R.; Spizzichino, S.; Lunazzi, L.; Mazzanti, A.; Schlosser, M. BValues as a Sensitive Measure of Steric Effects. *Chem. − Eur. J.* **2009**, *15*, 2645−2652.
(47) Patel, D. C.; Woods, R. M.; Breitbach, Z. S.; Berthod, A.; Armstrong, D. W. Thermal Racemization of Biaryl Atropisomers. *Tetrahedron: Asymmetry* **2017**, *28*, 1557−1561.

DOI: 10.1021/acsomega.9b00619
ACS Omega 2019, 4, 6044−6049